Title

A Critical Role of Inhibition in Temporal Processing Maturation in the Primary Auditory Cortex.

Journal

Cerebral Cortex, 28(5)

ISSN

1047-3211

Authors

Cai, Dongqin
Han, Rongrong
Liu, Miaomiao
et al.

Publication Date

2018-05-01

DOI

10.1093/cercor/bhx057

Peer reviewed

Cerebral Cortex, May 2018;28: 1610–1624

doi: 10.1093/cercor/bhx057
Advance Access Publication Date: 1 March 2017
Original Article

ORIGINAL ARTICLE

A Critical Role of Inhibition in Temporal Processing Maturation in the Primary Auditory Cortex

Dongqin Cai[1], Rongrong Han[1,2], Miaomiao Liu[1], Fenghua Xie[1], Ling You[1], Yi Zheng[3], Limin Zhao[4], Jun Yao[3], Yiwei Wang[1], Yin Yue[1], Christoph E. Schreiner[5] and Kexin Yuan[6]

[1]Department of Biomedical Engineering, School of Medicine, IDG/McGovern Institute for Brain Research, Tsinghua University, Beijing 100084, China, [2]Department of Otolaryngology, Weifang People's Hospital, Weifang, Shandong 261000, China, [3]State Key Laboratory of Biomembrane and Membrane Biotechnology, Tsinghua-Peking Joint Center for Life Sciences, School of Life Sciences, IDG/McGovern Institute for Brain Research, Tsinghua University, Beijing 100084, China, [4]Department of Otolaryngology, Affiliated Hospital of Weifang Medical University, Weifang, Shandong 261031, China, [5]Department of Otolaryngology, Kavli Center for Fundamental Neuroscience, University of California at San Francisco, California, MA 94158, USA and [6]Department of Biomedical Engineering, School of Medicine, IDG/McGovern Institute for Brain Research, Center for Brain-Inspired Computing Research, Tsinghua University, Beijing 100084, China

Address correspondence to Kexin Yuan, Room B218, School of Medicine, Tsinghua University, Haidian District, Beijing 100084, China.
Email: kexinyuan@tsinghua.edu.cn

Dongqin Cai and Rongrong Han contributed equally to this work

Abstract

Faithful representation of sound envelopes in primary auditory cortex (A1) is vital for temporal processing and perception of natural sounds. However, the emergence of cortical temporal processing mechanisms during development remains poorly understood. Although cortical inhibition has been proposed to play an important role in this process, direct in-vivo evidence has been lacking. Using loose-patch recordings in rat A1 immediately after hearing onset, we found that stimulus-following ability in fast-spiking neurons was significantly better than in regular-spiking (RS) neurons. In-vivo whole-cell recordings of RS neurons revealed that inhibition in the developing A1 demonstrated much weaker adaptation to repetitive stimuli than in adult A1. Furthermore, inhibitory synaptic inputs were of longer duration than observed in vitro and in adults. Early in development, overlap of the prolonged inhibition evoked by 2 closely following stimuli disrupted the classical temporal sequence between excitation and inhibition, resulting in slower following capacity. During maturation, inhibitory duration gradually shortened accompanied by an improving temporal following ability of RS neurons. Both inhibitory duration and stimulus-following ability demonstrated exposure-based plasticity. These results demonstrate the role of inhibition in setting the pace for experience-dependent maturation of temporal processing in the auditory cortex.

Key words: development, inhibition, plasticity, primary auditory cortex, rat

Introduction

Considering the transient nature of environmental and communication sounds, temporal processing is particularly important for the auditory system (Mauk and Buonomano 2004). Natural sounds such as human speech and animal vocalization are temporally modulated, and can be recognized

largely based on their temporal modulation patterns (Rosen 1992; Kanwal et al. 1994; Shannon et al. 1995; Wang et al. 1995; Ahissar et al. 2001; Nagarajan et al. 2002; Singh and Theunissen 2003). For modulation frequency within the ethological range, centered around 6–10 Hz in rodents (Liu et al. 2003; Kim and Bao 2009), these sounds are likely represented in the auditory cortex (ACx) by responses that are time locked to the stimuli envelopes (Ahissar et al. 2001; Joris et al. 2004).

Compared with adult humans, infants have a limited temporal sound resolution ability (Kuhl et al. 1997). Human psychophysical studies have also demonstrated a common association between impaired cortical temporal processing and auditory and language disabilities in children (Tallal et al. 1996; Wright et al. 1997; Nagarajan et al. 1999; Temple et al. 2001). Congenitally, deaf children who receive an early cochlear implant often develop significantly better cortical stimulus-following ability compared with those who receive an implant at later ages (Ponton et al. 1996, 1999; Shepherd et al. 1997), indicating a critical role of sensory experience in the maturation of cortical temporal processing. Recent animal studies revealed the developmental course of temporal processing in the cortex, and showed sensitivity to the acoustic environment not only for the maturation of spectral tuning and binaural integration (de Villers-Sidani et al. 2007; Polley et al. 2013), but that cortical representation of temporally modulated sounds is also profoundly influenced by early sensory experience (Chang and Merzenich 2003; Chang et al. 2005; Zhou and Merzenich 2008). However, the mechanisms underlying the experience-dependent development of cortical temporal responses remain unclear.

In the auditory system of rodents, thalamocortical connectivity largely matures at around P14 (Zhao et al. 2009; Barkat et al. 2011; Hackett et al. 2015), whereas cortical temporal response properties mature toward the end of the first postnatal month (Chang et al. 2005). This apparent time difference suggests a potential role of intracortical mechanism in the maturation of cortical temporal processing. Previous studies conducted both in vivo and in vitro reported a decrease in input resistance in the ACx of rodents from infancy to adulthood (Dorrn et al. 2010; Oswald and Reyes 2011), suggesting an even higher excitability of auditory cortical neurons in young brains. Therefore, the contribution of cellular excitability to the control of temporal response resolution in the developing A1 might be limited.

The role of inhibitory circuits in the functional maturation of sensory cortices has been extensively studied in the past decade (Hensch 2005; Sun 2007; Feldman 2009; Froemke and Jones 2011; Kullmann et al. 2012; Le Magueresse and Monyer 2013). Particularly, in the primary visual cortex, the level of inhibition increases to open and then close the critical period of ocular dominance plasticity. Inhibitory synapses in the ACx also have been demonstrated to be exceptionally dynamic during development (Sanes and Kotak 2011). Progressive, experience-dependent improvement of frequency-selectivity of inhibition appears instrumental for the maturation of auditory cortical synaptic receptive field (Dorrn et al. 2010, but also see Sun et al. 2010). How cortical inhibition changes may contribute to the development of cortical processing in temporal domain is still unclear. Extracellular studies of the development of the spectral and temporal response properties of auditory cortical neurons revealed a significantly stronger forward-masking effect in the developing A1 (after hearing onset) than in adult A1, suggesting inhibitory receptive fields of a prolonged temporal nature (Chang et al. 2005). Indeed, paired recordings between pyramidal and specific subtype of inhibitory neurons in Layers 2/3 of the developing ACx slice demonstrated inhibitory postsynaptic currents (IPSCs) with long duration (Kotak et al. 2008; Oswald and Reyes 2011; Takesian et al. 2012). However, in intact neural network, inputs from different subtypes of inhibitory neurons integrate to shape neural activity (Isaacson and Scanziani 2011). Therefore, the precise relationship between the duration of integrated inhibition and the development of cortical temporal processing needs to be clarified by direct evidence in vivo.

Here, we show that temporal response properties in the developing A1 of rats are cell-type specific with differences in dynamics. In particular, regular-spiking (RS) neurons demonstrated weaker stimulus-following ability compared with FS neurons. In-vivo whole-cell voltage-clamp recordings from RS neurons in both urethane and light-pentobarbital-anesthetized animals revealed that inhibitory input is long-lasting early in the developing A1 and gradually decreases toward adulthood. The initially longer duration of inhibition led to overlap and summation of inhibitory inputs evoked by 2 closely following stimuli. In addition, inhibition in the developing A1 demonstrated significantly weaker adaptation to repetitive stimuli than in the adult A1. These 2 inhibitory properties jointly limited the stimulus-following ability of RS neurons early in the developing A1. We then show that acoustic experience may accelerate the maturation of cortical temporal processing via exposure-induced shortening of inhibitory duration.

Materials and Methods

Animal Preparation

All experimental procedures were approved by the Institutional Animal Care and Use Committee at Tsinghua University, Beijing, China. Experiments were performed in a sound-attenuating chamber (IAC-Acoustics, UK). In experiments requiring anesthesia, Sprague-Dawley rat pups from P12 to P21, juvenile and adolescent rats from P22 to P35 and female adult rats (≥3 months old) were anaesthetized intraperitoneally with urethane (Cruikshank and Weinberger 1996; Li et al. 2013) (1.4 g/kg). For light-pentobarbital recordings in pups, pentobarbital (35 mg/kg) (de Villers-Sidani et al. 2007) was used for sedation and surgery. An initial injection of pentobarbital was generally sufficient for rat pups to undergo the surgical process without supplements. Once surgery was done, recordings were not started until rat pups demonstrated paw retraction and active whisking. The interval between pentobarbital injection and whole-cell recording was on average >3 h. Craniotomy and durotomy were performed to expose the cortex. The location of A1 in the right hemisphere was determined by extracellular recordings at ~500 μm below the pial surface using parylene-coated tungsten electrodes (1 MΩ, MicroProbes): A1 neurons fire action potentials at short latency to the characteristic frequency and are organized tonotopically from low to high frequency along the posterior–anterior axis (Polley et al. 2007). Our recordings targeted the depth range of 450–600 μm, the putative thalamic recipient layer. The temporal following capacities of cortical neurons were obtained with a pulsed-noise train (white noise, 5 ms duration, 1 ms ramp, 5 pulses per train), generated and calibrated by a TDT System 3 (Tucker-Davis Technologies), pseudorandomly presented at 5 repetition rates (2, 4, 7, 10, and 12.5 pps). Stimulus intensity was set at 20 dB above the threshold of each individual neuron recorded. The spiking threshold decreased from 40–60 dB at P12 to 20–30 dB in adults. Tones and noise pulses were delivered through a calibrated free-field speaker positioned contralateral to the recorded hemisphere.

Housing Condition of Animals

Mother rats and their pups (P11) were purchased from Weitonglihua Experimental Animal Co., Ltd (Beijing, China) and subsequently raised in the Laboratory Animal Research Center of Tsinghua University (SYXK, 2014-0024) with standard temperature, humidity and light/dark cycle conditions. The level of background noise in animal facility was around 40 dB sound pressure level (SPL), and no acoustic stimulation with particular pattern was detected.

In-Vivo Whole-Cell Voltage/Current-Clamp and Loose-Patch Recordings

In-vivo whole-cell recordings for both rat pups and adults were obtained from neurons located in the input layer described above. Cortical pulsations were prevented with 4% agar. Recordings were made with a MultiClamp 700B amplifier (Molecular Devices). The patch pipettes contained (in mM): 125 Cs-gluconate, 5 TEACl, 4 MgATP, 0.3 GTP, 10 phosphocreatine, 10 HEPES, 0.5 EGTA, 3.5 QX-314, 2 CsCl, and 1% biocytin (voltage clamp), or 135 K-gluconate, 5 NaCl, 5 MgATP, 0.3 GTP, 10 phosphocreatine, 10 HEPES, 0.5 EGTA (current-clamp and loose-patch), with pH 7.2. The impedance of patch pipettes was set to 4–6 MΩ for whole-cell recordings and 10 MΩ for loose-patch recordings. Whole-cell and pipette capacitances were partially or completely compensated and initial series resistance (Rs) (20–60 MΩ) was compensated for 50% to achieve an effective series resistance of 10–30 MΩ. Data were filtered at 5 kHz, digitized at 10 kHz and analyzed with Clampfit10 (Molecular Devices) and Matlab (MathWorks). Cells were excluded if either the initial resting membrane potential was less negative than −50 mV or Rs changed more than 30% over the entire experiment. To obtain sound-driven synaptic conductance, neurons were voltage-clamped at −70 mV and 0 mV, which are around the reversal potentials for inhibitory and excitatory currents, respectively. With a relatively large pipette tip, whole-cell recordings almost exclusively targeted pyramidal neurons (Supplementary Fig. 1*A–C*), consistent with the report that most excitatory neurons in Layer 4 of the rat ACx are pyramidal (Barbour and Callaway 2008). However, we did occasionally record from non-pyramidal neurons (Supplementary Fig. 1*D*). The morphologies of the recorded neurons were constructed with the standard histological procedure of biocytin staining. Voltage-clamp quality was considered to be reasonably good, based on the linearity of the current–voltage curves. This was further confirmed by the absence of significant excitatory currents when the neuron was clamped at 0 mV (Fig. 5*A*). For current-clamp recordings, similar glass pipettes were used. Loose-patch recordings were performed under voltage-clamp mode with pipettes containing the solution for the current-clamp. After a 100–400 MΩ seal was formed, the spike signal was filtered at 10 kHz and sampled at 20 kHz. Recordings of spikes evoked by various repetition rates were repeated 5–10 times for each neuron, and the spike number evoked by the same repetition rate was averaged.

Cell Type

Cell-type classification was made for spikes recorded in cell-attached mode. Based on the inspection of the shape of action potentials and spiking patterns, recorded neurons were categorized into 2 types. The first type had relatively small upward peaks and longer trough-to-peak intervals (Fig. 2*A*,*B*, insets), defined as the time interval between the peak of the action potential and the peak of the after-hyperpolarization. These neurons usually exhibited single-spike responses when stimulated with a brief stimulus. The second type had larger upward peaks and shorter trough-to-peak intervals (Fig. 3*A*,*B*, insets). These neurons often demonstrated a train of APs when stimulated. We categorized neurons with trough-to-peak intervals ≥0.45 ms as RS (putative pyramidal) neurons and those with trough-to-peak intervals <0.45 ms as FS (putative inhibitory) neurons (Cardin et al. 2007; Niell and Stryker 2008; Moore and Wehr 2013). The average trough-to-peak interval for RS and FS neurons in young animals was 0.96 ± 0.22 ms (mean ± SD; n = 30) and 0.27 ± 0.08 ms (mean ± SD; n = 6), respectively, and in adult animals was 0.89 ± 0.19 ms (mean ± SD; n = 30) and 0.19 ± 0.04 ms (mean ± SD; n = 6), respectively (Fig. 4*A*). Although the chance of encountering FS neurons was very low when the recording pipette had an impedance of <6 MΩ (Sun et al. 2013), we did encounter neurons histologically identified as non-pyramidal (Supplementary Fig. 1*D*). Only Layer 4 neurons were included for data analysis.

Spike Threshold

Spike threshold was calculated as the membrane potential that corresponded to the maximum of the second derivative of the membrane voltage between the baseline and peak of the action potential minus the resting membrane potential.

Spiking Probability

Spiking probability was defined as the number of occurrence of spike responses to the first pulse in each trial divided by the total number of trials.

Relative Delay Between Excitation and Inhibition

Relative delay was calculated as the onset latency of inhibitory synaptic response evoked by the first pulse at 2 pps minus the excitation onset latency.

Stimulus-Following Ability

To determine the stimulus-following ability for each neuron, trains of 5 white noise pulses (5 ms duration, 1 ms ramp, 20 dB SPL above threshold) were delivered 6 times at each of the 5 repetition rates (2, 4, 7, 10, and 12.5 pps) for whole-cell and loose-patch recordings. To minimize adaptation effects, repetition rates were pseudorandomly interleaved. Since the interval between the onsets of 2 pulse trains was fixed at 6 s, sequential trains were separated by at least 1.5 s of silence. To minimize the influence of spontaneous activity to stimulus-evoked response counting, the estimated number of spontaneous spikes was subtracted. For loose-patch recordings, the response magnitude to each noise pulse was quantified as the average number of spikes activated (7–40 ms after stimulus onset for adults; 20–50 ms for rat pups) minus the estimated number of spontaneous spikes during this period. Spontaneous spiking or synaptic activity was estimated during the last 1 s of the ~5.7 s quiet period following each 12.5 pps sweep (Bao et al. 2004). The average number of spontaneous spikes in young and adult animals was 0.9 and 3.5 per second, respectively. For whole-cell recordings, noise-evoked synaptic responses were identified according to their onset latencies and peak amplitudes. The response onset latency was identified during the rising phase of the response trace at the time point where the peak conductance change was 3-fold of the SD of the baseline fluctuation. Only synaptic responses with latencies within 7–40 ms for

adults and 20–50 ms for the rat pups from the onset of stimulus were considered. The normalized spike response at each repetition rate was calculated as the average spike number to the last 4 noise pulses divided by the spike number evoked by the first noise pulse. The normalized synaptic response at each repetition rate was calculated as average synaptic response magnitude to the last 4 noise pulses divided by the response magnitude of the first noise pulse. The repetition-rate transfer function is the normalized cortical response as a function of the noise-pulse rate. Thus, a normalized response of one indicates that, at the given repetition rate, each of the pulses in the train, on average, evoked the same number of spikes or had the same synaptic current amplitude as the first pulse. A response greater than 1 indicates facilitation, while that less than 1 indicates adaptation.

Conductance

Excitatory synaptic conductance $G_e(t)$ and inhibitory synaptic conductance $G_i(t)$ at any time point t were derived using:

$$I(t) = G_r(V(t) - E_r) + G_e(t)(V(t) - E_e) + G_i(t)(V(t) - E_i)$$

where $I(t)$ is the amplitude of synaptic current, and E_e (0 mV) and E_i (−70 mV) are the reversal potentials of the excitatory and inhibitory synaptic conductance, respectively. In this study, a corrected clamping voltage was used, instead of the holding voltage applied (V_h). $V(t)$ was corrected as $V(t) = V_h - R_s \times I(t) V(t) = V_h - R_s \times I(t)$, where R_s is the effective series resistance. Junction potentials were not corrected in the current study. Resting conductance G_r was derived using $I_r(V_h) = G_r(V_h - E_r)$, where E_r is the resting membrane potential. G_r and E_r were 2 unknowns solved by measuring I_r at 2 different V_h. By holding the voltage at 2 different values, $G_e(t)$ and $G_i(t)$ were calculated at any t. They reflected the strengths of pure excitatory and inhibitory synaptic inputs, respectively.

Decay Time Constant

The time constant for the decay phase of the postsynaptic current (PSC) at 2 pps was obtained by fitting the current between the peak and 500 ms after stimulus onset to the function $I(t) = Ae^{-t/\tau} + C$. All fittings were performed using Levenberg–Marquardt, nonlinear least-square algorithm in Clampfit10 (Molecular Devices). In cases where the decay phase could not be fitted using an exponential function, the absolute time it took to decrease from the peak to 37% peak amplitude was used as a measurement for the decay time constant.

Measurement of Series Resistance and Input Resistance

Following a 3-s equilibration period after the response to a brief noise pulse of 70 dB (with clamping at 0 mV), a 10-mV voltage step was delivered to calculate series and input resistance. The traces were repeated 4–6 times before being averaged. After voltage step injection, the current increases to an initial transient peak $I_{peak} = V_{step}/R_{series}$, then falls exponentially with decay constant $\tau \approx R_{series}C_m$ to a steady value of $I_{steady} = V_{step}/(R_{series} + R_{input})$. In this way, series resistance was computed by dividing the amplitude of the voltage step by the peak current transients, while input resistance was estimated by subtracting the amplitude of the voltage step divided by the steady current from t-series resistance.

Statistical Analysis

Statistical analysis was performed using GraphPad Prism 6 software (GraphPad Software, Inc.). The Shapiro–Wilk test was first applied to examine whether samples had normal distribution. In the case of normal distribution, t-test or analysis of variance was applied. Otherwise, a non-parametric test (Mann–Whitney U or Wilcoxon signed-rank tests) was applied. In multiple comparison situations, Bonferroni and Dunn's were chosen as post-hoc tests for one-way ANOVA and the Kruskal–Wallis H-test, respectively. All tests were two-tailed with alpha = 0.05. Statistical significance is indicated as $^{*}P < 0.05$, $^{**}P < 0.01$, $^{***}P < 0.001$, $^{****}P < 0.0001$, n.s. $P > 0.05$.

Histology

After at least 5 min of whole-cell recordings, some neurons were histologically recovered to show their cell types and laminar distribution. Briefly, the recording pipette containing biocytin was pulled off the cell gently or in a shearing direction (perpendicular to the direction approaching the cell) to avoid cell damage. Within 1 h of the completion of labeling, animals were sacrificed with an overdose of urethane and then perfused with saline and 4% paraformaldehyde in phosphate-buffered saline with 0.2% picric acid. Brains were postfixed in 4% paraformaldehyde overnight at 4°C and cryoprotected with 30% sucrose. Coronal sections (40–50 μm) were cut with a freezing cryostat (Leica CR 1900) and then reacted with cyanine 3 (Cy3)-streptavidin (1:500, Jackson ImmunoResearch). Images of fluorescently labeled cells were acquired by a confocal microscope (Carl Zeiss LSM 510 Meta) using 10× air, 40× water, or 60× oil-immersion objective and processed by Adobe Photoshop software. Under the experimental conditions, ~50% of recovered cells exhibited adequate intracellular filling with Biocytin, as evidenced by relatively complete somatic and dendritic morphologies in Supplementary Figure 1.

Results

Temporal Processing Capacity in the Developing A1 is Cell-Type Specific

We examined the stimulus-following ability of neurons in the developing (postnatal day (P) 12–21; P12, hearing onset; $n = 36$) and mature (≥3 months, $n = 36$) rat A1 using in-vivo loose-patch recordings (Fig. 1A). Animals were anesthetized with urethane. Our recordings targeted the depth range of 450–600 μm, the putative thalamic recipient Layer 4. To avoid potential bias due to immature thalamocortical connectivity (Zhao et al. 2009; Barkat et al. 2011; Hackett et al. 2015), we constrained our recordings to the A1 area that showed reliable tonal-driven responses with short latency. Trains of 5 white-noise pulses presented at repetition rates commonly found in natural animal vocalizations (Kim and Bao 2009) were used to probe the temporal resolution of cortical responses (Fig. 1B). Considering the potential influences of variance in response threshold, stimulus intensity was set at 20 dB above the minimum threshold of each individual neuron recorded.

Based on the shape of action potentials and spiking patterns, recorded neurons were categorized into 2 types. The first type had relatively small upward peaks and longer peak-to-peak intervals (Fig. 2A,B, insets), defined as the time interval between the peak of the action potential and the peak of the after-hyperpolarization. These "RS" neurons usually exhibited single-spike responses when stimulated with a brief stimulus. The second type had larger upward peaks and shorter trough-to-peak intervals (Fig. 3A,B, insets). These "fast-spiking"

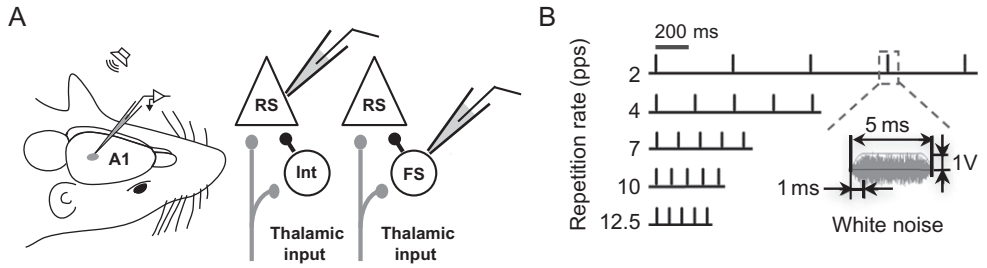

Figure 1. Schematic of electrophysiological recordings from the developing primary ACx (A1). (*A*) Loose-patch recordings from RS and FS neurons in Layer 4 in vivo. (*B*) Trains of white-noise pulses with various repetition rates (2–12.5 pps [pulse per second]) were used to characterize the temporal response resolution of cortical neurons. The voltage amplitude corresponds to sound intensity of 80 dB SPL.

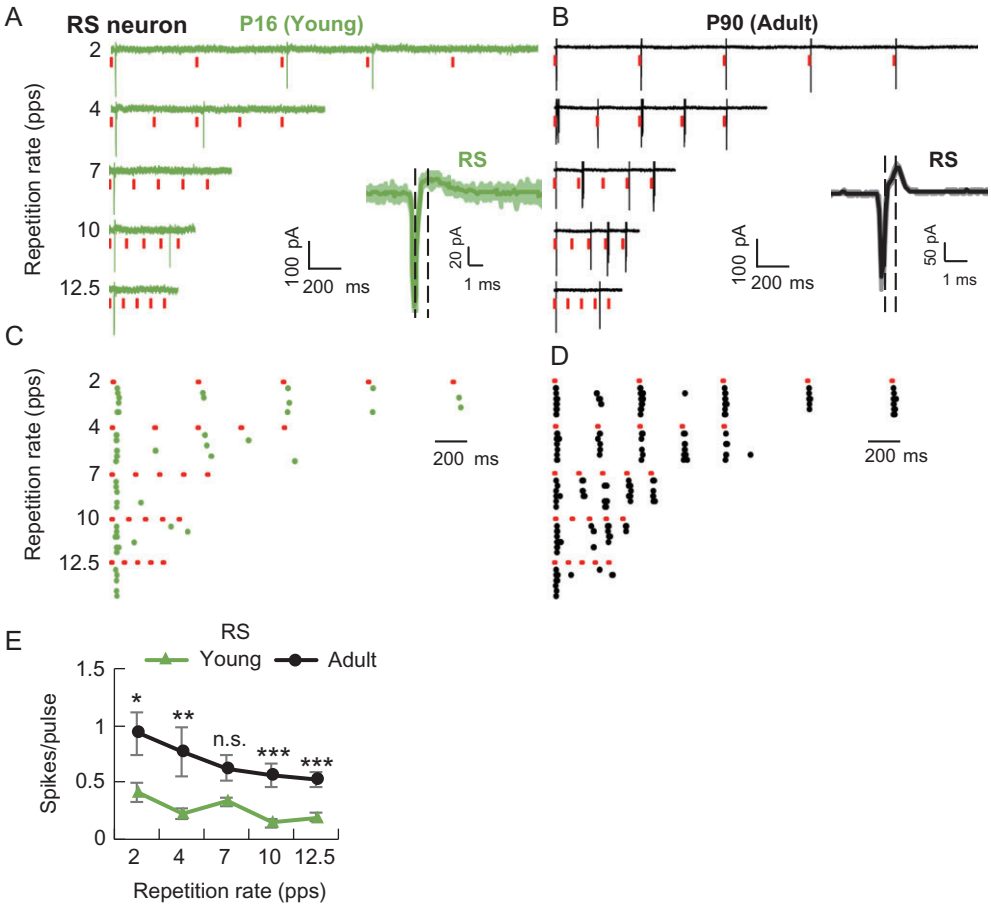

Figure 2. Regular-spiking (RS) neurons in the developing A1 demonstrated poor stimulus-following ability compared with that in adult A1. (*A* and *B*) Respective temporal responses of P16 and P90 RS neurons. Red bars, stimulus pulses. Insets, light color, superimposed individual spikes; dark color, average spike; vertical line, indication of trough and peak time in the action potential. (*C* and *D*) Raster plots corresponding to neurons in (*A*) and (*B*). (*E*) Number of spikes evoked by each stimulation pulse in RS neurons. Young, $n = 30$; adult, $n = 30$. Data in (*E*) are means ± SEM (error bars). Mann–Whitney *U*-test (*$P < 0.05$; **$P < 0.01$; ***$P < 0.001$; n.s. $P > 0.05$).

neurons often demonstrated a train of APs when stimulated. We categorized neurons with trough-to-peak intervals >0.45 ms as RS neurons (putative pyramidal; pup, $n = 30$; adult, $n = 30$) and those with trough-to-peak intervals ≤0.45 ms as FS neurons (putative inhibitory; pup, $n = 6$; adult, $n = 6$), consistent with other studies (Cardin et al. 2007; Niell and Stryker 2008; Moore and Wehr 2013). The average trough-to-peak interval for RS and FS neurons in young animals was 0.96 ± 0.22 and 0.27 ± 0.08 ms, respectively, and in adult animals 0.89 ± 0.19 and 0.19 ± 0.04 ms (Fig. 4A). FS neurons, as identified here, are most likely GABAergic interneurons although some non-GABAergic neurons fire narrow spikes as well (Dykes et al. 1988; Gray and McCormick 1996).

RS neurons in the developing A1 adapted strongly to repetitive stimuli and demonstrated much weaker stimulus-following ability than those in adults (Fig. 2A–D). This was further confirmed by the normalized spike response (Bao et al. 2004; Chang et al. 2005; Imaizumi et al. 2010), defined as the average spike count to the last 4 noise pulses divided by the count for the first noise pulse (Fig. 4B, left). Interestingly, there

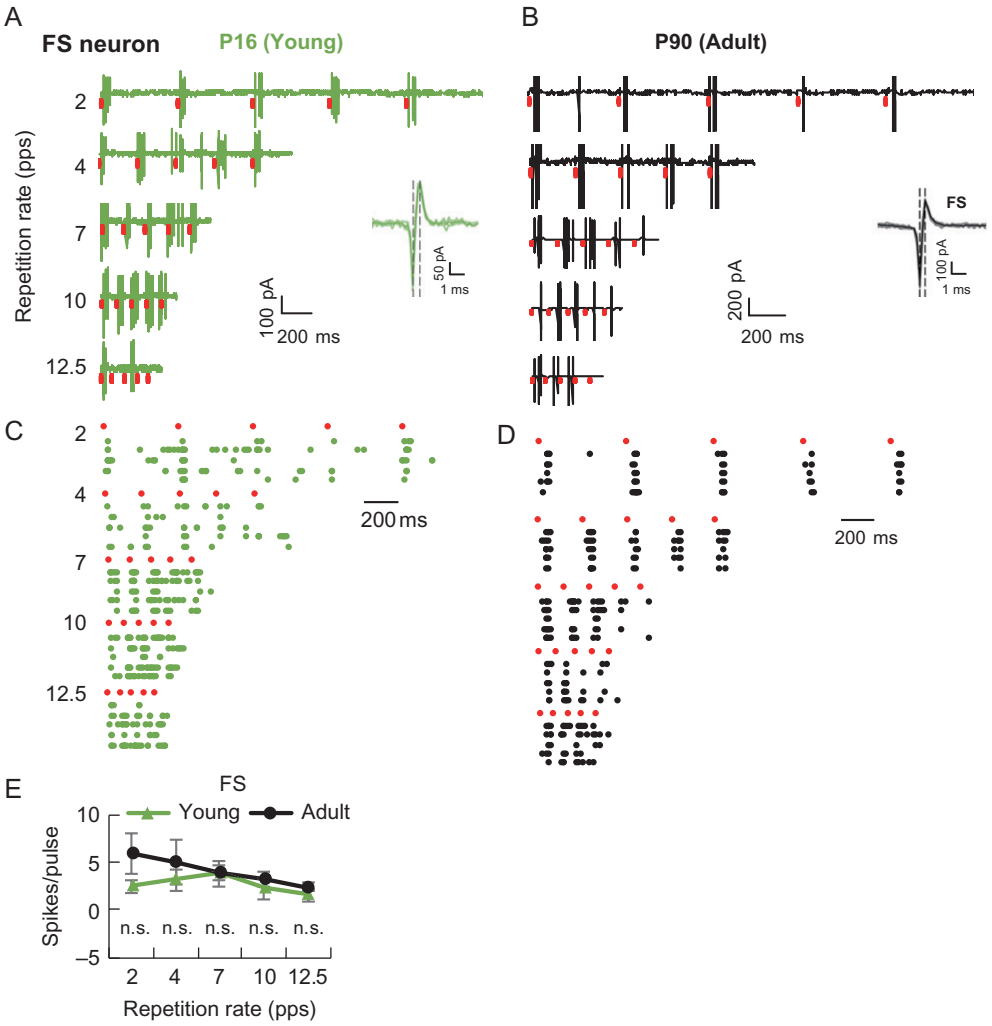

Figure 3. FS neurons in both developing and adult A1 exhibited superior stimulus-following ability. (*A* and *B*) Respective temporal responses of P16 and P90 FS neurons. Red bars, stimulus pulses. Insets, light color, superimposed individual spikes; dark color, average spike; vertical line, indication of trough and peak time in the action potential. (*C* and *D*) Raster plots corresponding to neurons in (*A*) and (*B*). (*E*) Number of spikes evoked by each stimulation pulse in FS neurons. Data are means ± SEM (error bars). Young, $n = 6$; Adult, $n = 6$. Mann–Whitney *U*-test (n.s. $P > 0.05$).

was no significant difference between the 2 age groups in spiking probability, calculated as the number of occurrence of spike responses to the first pulse in each trial divided by the total number of trials (Fig. 4*B*, right). In contrast, FS neurons faithfully followed repetitive stimuli equally for both age groups (young, $n = 6$; adult, $n = 6$; Figs 3*A–D* and 4*C*). RS neurons in the developing A1 fired fewer spikes than those in the adult A1 (Fig. 2*E*), while there was no significant difference for FS neurons (Fig. 3*E*). Given the well-characterized feed-forward thalamocortical projection system (Isaacson and Scanziani 2011), thalamocortical afferents should equally drive FS and RS neurons, yet, their temporal following capacity differed, suggestive of distinct cellular and/or network effects on the temporal response of these cell types. Thus, the temporal response property in the developing A1 was cell-type specific.

Inhibition Restrains Temporal Processing Capacity of RS Neurons in the Developing A1

What mechanisms underlie the poor stimulus-following ability of RS neurons in the developing A1? We performed in-vivo whole-cell voltage-clamp recordings from Layer 4 A1 neurons of both age groups (young, $n = 48$; adult, $n = 37$) (Fig. 5*A*, left). The pipette impedance for whole-cell recording was <6 MΩ. To obtain sound-driven synaptic conductance, neurons were voltage clamped at −70 and 0 mV, which are around the reversal potentials for inhibitory and excitatory currents, respectively (Tan et al. 2004). Voltage-clamp quality was considered to be reasonably good, based on the linearity of the current–voltage (*I–V*) curves (Fig. 5*A*, right). This was further confirmed by the absence of significant excitatory currents when the neuron was clamped at 0 mV (Fig. 5*A*, middle). Eleven of the recorded neurons were labeled with biocytin. Consistent with previous report (Sun et al. 2013), the whole-cell recordings with large tip sizes (impedance < 6 MΩ) targeted almost exclusively pyramidal neurons in Layer 4 ($n = 10$, 4 neurons with relatively intact dendritic trees are shown in Fig. 5*B* and Supplementary Fig. 1*A–C*), but we did record from one neuron of non-pyramidal type (Supplementary Fig. 1*D*), which was not included in our data analysis. This does not exclude the possibility that a very small portion of non-pyramidal neurons was included in the data analysis.

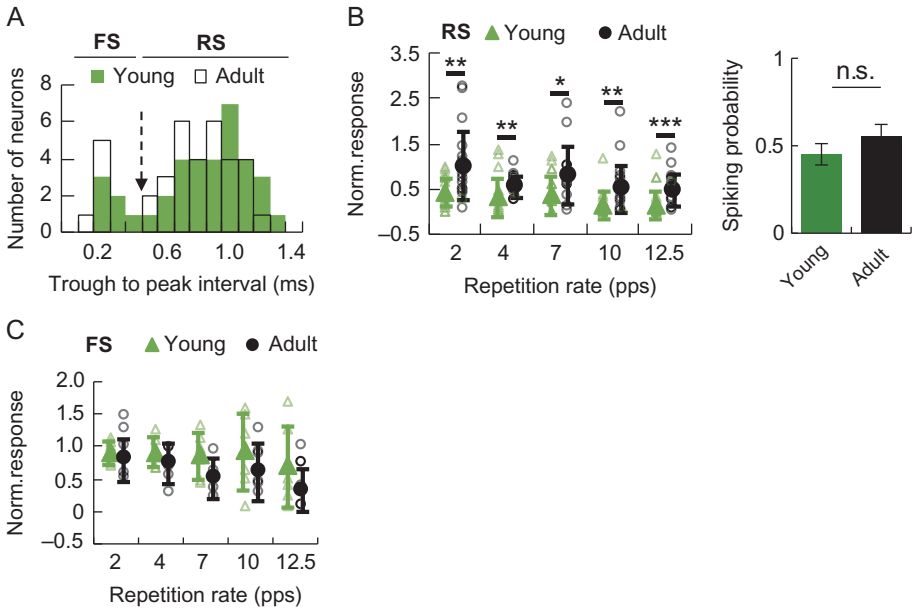

Figure 4. Characterization of the adaptation of RS and FS neurons across different repetition rates. (*A*) Distribution of average trough-to-peak intervals of action potential for young ($n = 36$) and adult ($n = 36$) neurons. RS (young, $n = 30$; adult, $n = 30$) and FS (young, $n = 6$; adult, $n = 6$) neurons were well separated according to the trough-to-peak intervals (young, RS: 0.96 ± 0.22 ms, FS: 0.27 ± 0.08 ms; adult, RS: 0.89 ± 0.19 ms, FS: 0.19 ± 0.04 ms). (*B*) Left, adaptation indicated by normalized responses of RS neurons across different repetition rates. Green hollow triangles, individual neurons from young animals; black hollow circles, individual neurons from adult animals; green solid triangles, mean value from young animals; black solid circles, mean value from adult animals. Right, comparison of spiking probability between the 2 age groups. Young, $n = 22$; adult, $n = 22$. (*C*) Adaptation indicated by normalized responses of FS neurons across different repetition rates. Data in (*B*) (Left) and (*C*) are means ± SD (error bars). Statistical analysis is Mann–Whitney *U*-test. Data in (*B*) (right) is means ± SEM (error bars). Statistical analysis is unpaired *t*-test (*$P < 0.05$; **$P < 0.01$; ***$P < 0.001$; n.s. $P > 0.05$).

We used single stimulus pulses to accurately measure the decay of inhibition (Supplementary Fig. 2*A*). Repetitive stimuli evoked inhibitory inputs with significantly longer time courses in the developing A1 than in the adult (young, 94 ± 11 ms, $n = 48$; adult, 20 ± 3 ms, $n = 37$; Fig. 5*C–E*). The inhibitory decay time recorded in developing A1 in vivo was significantly longer than that reported in vitro (Kotak et al. 2008; Oswald and Reyes 2011). Data from light-pentobarbital animals will be presented near the end of the Result section to show that this difference was not urethane-specific. The prolonged inhibition in rat pups led to an overlap of inhibitory inputs evoked by 2 closely spaced, consecutive stimulus pulses (Fig. 5*C*, inset) for repetition rates faster than 2 pps. This overlap and summation of inhibition disrupted the typical temporal sequence between excitatory and inhibitory synaptic inputs (Wehr and Zador 2003), specifically, significant inhibition from the first pulse was already present before the arrival of excitation from consecutive pulses. This result was further confirmed by the normalized integral area, calculated as the total area under the curve of synaptic responses divided by the peak conductance at each repetition rate (Supplementary Fig. 2*B*). The integrated inhibition for pups exceeded that in the adult for all repetition rates. By contrast, excitatory areas were not different between the 2 groups. The peak conductance of both inhibition and excitation tended to be larger in the developing A1 than in the adult A1, yielding a higher *I*:*E* ratio. However, these differences did not reach significance in our sample (Fig. 5*F*). Inhibitory decay time decreased gradually between P12 and P26 (Fig. 6*A*), while excitatory decay time reached adult levels already by P18 (Fig. 6*B*). The decrease of *I*:*E* ratio was not significant, which is consistent with that reported in 2 earlier in-vivo studies (Dorrn et al. 2010; Sun et al. 2010) (Fig. 6*C*). These observations are compatible with the developmental changes observed in extracellular following properties obtained for RS neurons (Fig. 2).

As stated above, we constrained whole-cell recordings to the A1 area that demonstrated robust tonal-driven responses, and thalamocortical connectivity in the auditory system of rodents largely matures at around P14 (Zhao et al. 2009; Barkat et al. 2011; Hackett et al. 2015). With these 2 constraints, our data did not show significantly stronger depression of thalamic inputs to RS neurons in the developing A1 (Fig. 5*G*). Normalized synaptic response strength (averaged last 4 pulse responses/first pulse response) indicated that the excitatory inputs to RS neurons in both the developing and adult A1 faithfully followed repeated stimuli. Conversely, we observed significantly stronger adaptation of inhibitory inputs in the adult A1 than in the developing A1 from 4 to 10 pps (Fig. 5*C*), indicating that stronger inhibition is maintained in the developing A1 in response to repetitive stimuli.

The onset latency of both excitation and inhibition in the developing A1 was significantly longer than that in the adult A1 (Fig. 5*H*). It is unlikely that the late onset of excitation (24.48 ± 1.33 ms) in the young A1 would have impeded stimulus following because the smallest interval between consecutive pulses was 80 ms at 12.5 pps. In addition, the relative delay between excitation and inhibition was significantly larger in the developing A1 (young, 2.68 ± 0.50 ms, $n = 22$; adult, 0.77 ± 0.47 ms, $n = 22$) (Fig. 5*H*), which was generally consistent with that reported in another in-vivo whole-cell study (Dorrn et al. 2010). Since, theoretically, a larger relative delay of inhibition would result in stronger spiking activity, it is unlikely that it contributed to the poor stimulus-following ability in the developing A1.

Comparison of the intrinsic properties of RS neurons between the 2 age groups (young, $n = 15$; adult, $n = 10$) demonstrated that the resting membrane potential in the developing A1 was more

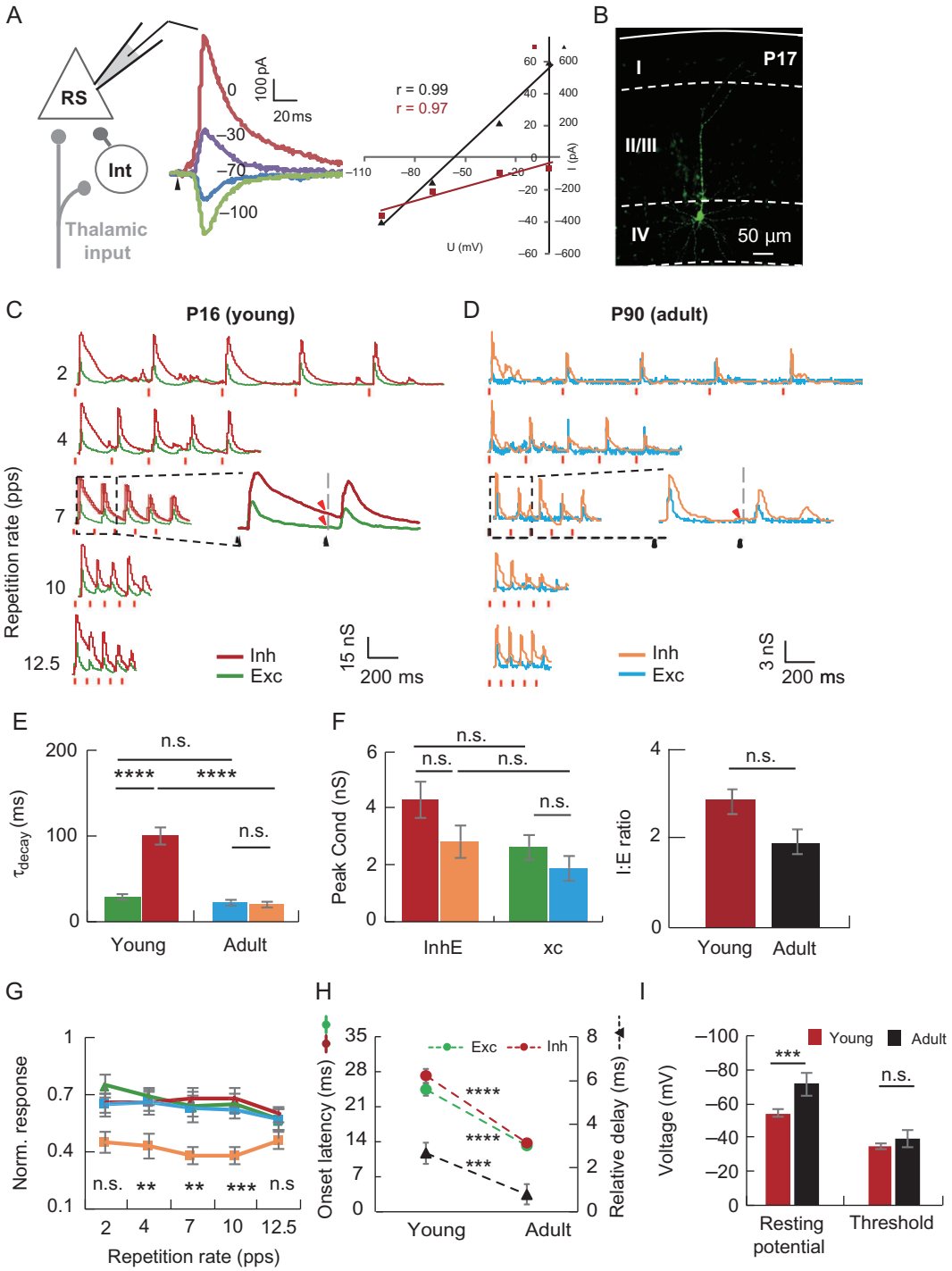

Figure 5. Inhibition restrains temporal processing capacity of RS neurons in the developing A1. (*A*) Left, schematic of in-vivo whole-cell recordings from RS neurons. Middle, synaptic currents recorded at different holding potentials from the same neuron. Black arrowhead, onset of stimuli. Right, *I–V* curves for synaptic currents averaged within 1–2 ms (red) and 21–22 ms (black) windows after response onset. (*B*) A Layer 4 pyramidal neuron in a P17 rat labelled during in-vivo whole-cell recording. Solid line, pial surface. Dashed lines, layer borders. (*C* and *D*) Synaptic temporal inhibition (Inh) and excitation (Exc) evoked in P16 and P90 neurons, respectively. Insets, magnified view of synaptic conductance at 7 pps. Vertical dashed line, onset of second stimulus pulse (all magnified views below conform to this description). (*E* and *F*) Comparison of decay time constant (τ_{decay}), peak amplitude of synaptic conductance and the *I:E* ratio between young and adult rats. Mann–Whitney *U*-test. Young, $n = 48$; adult, $n = 37$. (*G*) Adaptation of synaptic responses at each repetition rate indicated by normalized response. One-way ANOVA with Bonferroni post-hoc test (**$P < 0.01$; ***$P < 0.001$; n.s. $P > 0.05$). Young, $n = 48$; adult, $n = 37$. (*H*) Comparison of onset latency and the delay of inhibition relative to excitation between the 2 age groups. Young, $n = 22$; adult, $n = 22$. Statistical analysis is Mann–Whitney *U*-test. (*I*) Comparison of resting membrane potential and firing threshold between the 2 age groups. Young, $n = 15$; adult, $n = 10$. Statistical analysis is the Mann–Whitney *U*-test (***$P < 0.001$; n.s. $P > 0.05$). Data in (*E*) to (*G*) are means ± SEM (error bars). Colors in (*E*), (*F*), and (*G*) share the same meaning as those in (*C*) and (*D*).

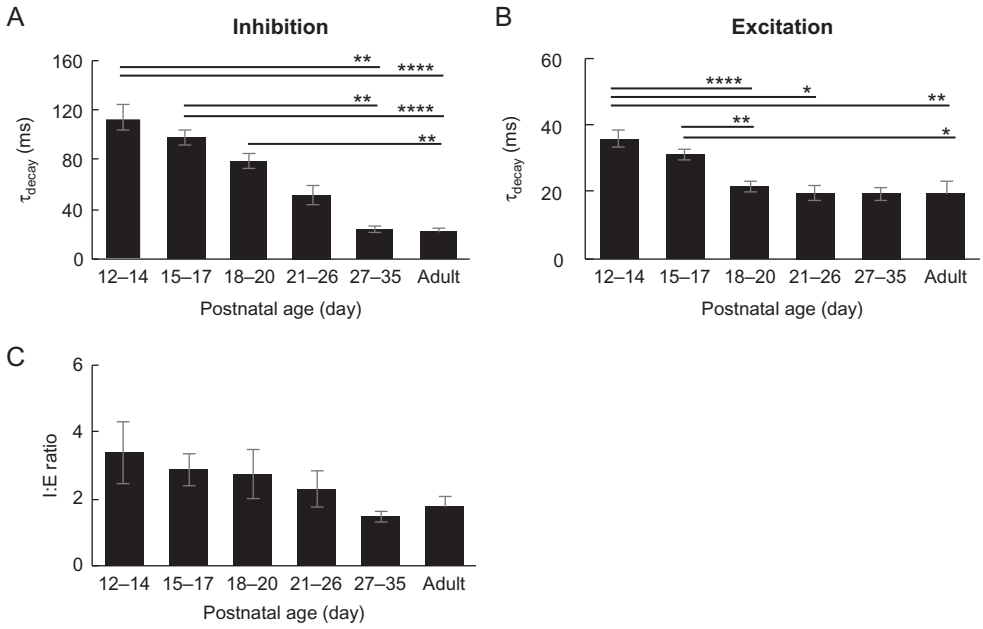

Figure 6. Maturational course of synaptic decay time and the *I:E* ratio during development. (*A* and *B*) Developmental change in inhibitory and excitatory decay times. (*C*) Developmental change in the *I:E* ratio. P12–14, $n = 10$; P15–17, $n = 7$; P18–20, $n = 10$; P21–26, $n = 4$; P27–35, $n = 6$; adult, $n = 18$. Data are means ± SEM (error bars). Kruskal–Wallis test with Dunn's multiple comparisons test (*$P < 0.05$; **$P < 0.01$; ****$P < 0.0001$; n.s. $P > 0.05$).

depolarized, which is generally consistent with in-vitro results (Oswald and Reyes 2008). Firing threshold was not significantly different between young and adult animals (Fig. 5*I*). Previous studies, conducted both in vivo and in vitro, reported a decrease in input resistance in the ACx of rodents from infancy to adulthood (Dorrn et al. 2010; Oswald and Reyes 2011), compatible with a higher excitability of auditory cortical neurons in young brains and incompatible with the observed lower responsiveness early in development. Therefore, intrinsic properties alone may not account for the limited temporal response resolution of RS neurons in the developing A1.

Our results demonstrate that integrated inhibitory inputs to single RS neurons in the developing A1 play an essential role in controlling stimulus-following ability, and verify the influence of inhibition on the maturation process as hypothesized in previous studies (Chang et al. 2005; Oswald and Reyes 2011).

Exposure Improves Temporal Processing Capacity and Shortens Inhibition Duration in the Developing A1

Both human and animal studies have shown that the development of auditory cortical temporal processing is experience dependent (Ponton et al. 1996; Chang and Merzenich 2003). To determine how sensory experience influences temporal processing plasticity in the developing A1, we exposed rat pups at P15 to noise pulses repeated at 20 pps, approximately at the high end of the repetition rates of animal vocalizations (Kim and Bao 2009), for 5 min during in-vivo loose-patch or whole-cell current-clamp recordings. The selection of the time course of 5 min was determined by the fact that most cells could not be held for more than 15 min due to the pulsation of the brain. Surprisingly, brief exposure was sufficient to improve the temporal response resolution of RS neurons for 4 and 7 pps (Fig. 7*A–D*), evidenced by significantly enhanced trial-by-trial reliability and weakened adaptation (Fig. 7*E*). In contrast, exposure did not induce any significant change in the adult A1 (Supplementary Fig. 3). These data suggest a high sensitivity of temporal processing in the developing A1 to sensory experience even for such a short and somewhat unnatural exposure.

What mechanisms could account for the temporal processing plasticity rapidly induced by brief sound exposure? We examined the effect of exposure on synaptic inputs. A few minutes of exposure significantly reduced the temporal summation of inhibition in the developing A1 by shortening inhibition duration (Fig. 8A, left). In contrast, magnitude and duration of excitatory responses were largely unchanged. Quantitatively, the decay time constant of inhibition decreased from 108 ± 21 to 63 ± 13 ms, whereas that of excitation remained the same (Fig. 8*B*). These results were confirmed for inhibition and excitation by the change in normalized integral area induced by exposure (Fig. 8*C*). To characterize how long after exposure plasticity effect could be observed, we recorded from cells before and at different time points after exposure ($n = 26$). A decrease in the inhibitory decay constant after only 5 min of exposure was maintained for at least 1 h (Fig. 8*D*). Exposure of pups resulted in no significant change in the peak conductance of inhibition and in the *I:E* ratio (Fig. 8*E*,*F*). Conversely, exposure did not induce any significant change in both decay constant and *I:E* ratio in the adult A1 (Supplementary Fig. 4).

The 5-min exposure time was necessitated by the limited holding stability of a neuron in vivo. To assess whether longer exposure time would impose a more enduring effect on inhibition decay constant and *I:E* ratio, we first pre-exposed a group of rat pups to 20 pps stimulation for 30 min, then obtained whole-cell recordings >12 h after exposure. This longer exposure also resulted in a significantly decreased inhibition decay constant that was maintained for >24 h (Fig. 8*G*,*H*) and tended toward a decrease in *I:E* ratio, although this difference did not reach statistical significance (Fig. 8*I*). These data demonstrate a strong and long-lasting effect of exposure to temporally modulated stimulus on the duration of inhibition during the maturational period, emphasizing the relevance of proper sound

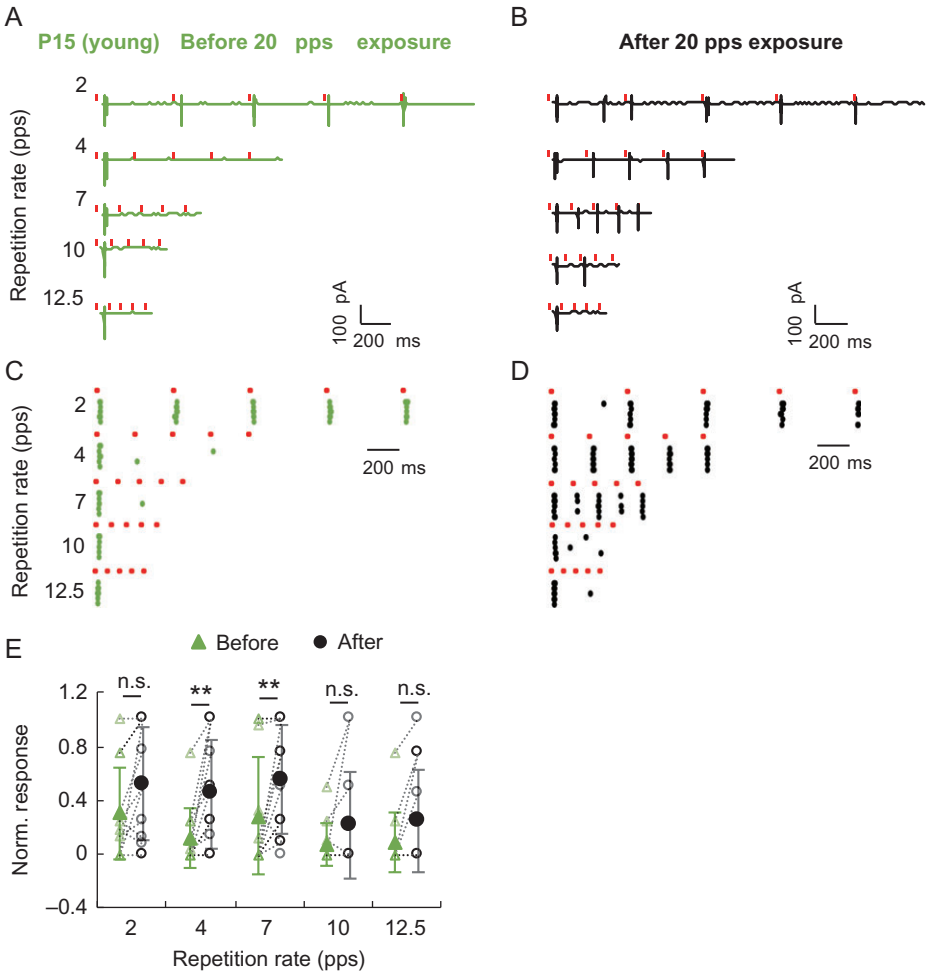

Figure 7. Exposure significantly improves the stimulus-following ability of RS neurons in the developing A1. (*A* and *B*) Effect of 5 min of exposure at 20 pps on temporal responses of a P15 neuron. (*C* and *D*) Raster plots of the representative neuron shown in (*A*) and (*B*); (*E*) Adaptation indicated by the normalized responses of young RS neurons before and after 20 pps exposure across different repetition rates, $n = 14$, 5 recorded by current-clamp recordings and 9 by loose-patch recordings. Green hollow triangles, individual neurons before exposure; black hollow circles, individual neurons after exposure; green solid triangles, mean value before exposure; black solid circles, mean value after exposure. Dashed lines, connecting the same neurons before and after exposure. Statistical analysis is means ± SD (error bars). Wilcoxon matched-pairs signed-rank test (**$P < 0.01$; n.s. $P > 0.05$).

statistics during development for achieving full hearing capacity (Kotak et al. 2008; Park et al. 2015; Khavarghazalani et al. 2016).

In addition to synaptic properties, we also examined the potential effect of exposure during development on cellular intrinsic properties using current-clamp recordings. Neither resting membrane potential nor firing threshold of RS neurons in the developing A1 was significantly changed by exposure (Fig. 9*A*). Input and series resistances, measured with a hyperpolarizing voltage of 10 mV and 100 ms duration (Fig. 9*B*), were not altered by exposure (Fig. 9*C*). Thus, these results suggest that both excitability of neurons and our recording quality likely did not contribute to the observed exposure-induced improvement of temporal processing ability in the developing A1.

To assess the potential influence of the type of anesthesia used in these experiments (urethane), we obtained whole-cell recordings in lightly pentobarbital-anesthetized rat pups. Recording commenced more than 3 h after the last injection with the agent, resulting in a nearly waking condition of the animals (see Materials and Methods). The decay of inhibition in light-pentobarbital animals was similar to that measured in the urethane group. Five minutes of sound exposure significantly shortened the duration of inhibition but not the *I*:*E* ratio (Supplementary Fig. 5). These data confirm that prolonged time course of inhibition in the developing A1 was not urethane-specific and was readily shaped by sensory experience. A previous study in vitro reported that hearing loss, that is, a lack or reduction of sound exposure during maturation, prevented the reduction of IPSC duration (Kotak et al. 2008). Our results provide direct evidence that acoustic experience can alter and, actually, accelerate maturational changes of IPSC duration in vivo.

Discussion

Sensory cortical networks operate through an equilibrium of recurrent excitation and inhibition (Monier et al. 2003). Understanding the developmental processes that govern the refinement of cortical circuits is essential for identifying developmental inadequacies that can result in sensory impairments and disorders. Intracortical inhibition, mediated by GABAergic interneurons, plays a critical role in timing of cortical maturation (Hensch 2005; Le Magueresse and Monyer 2013). We

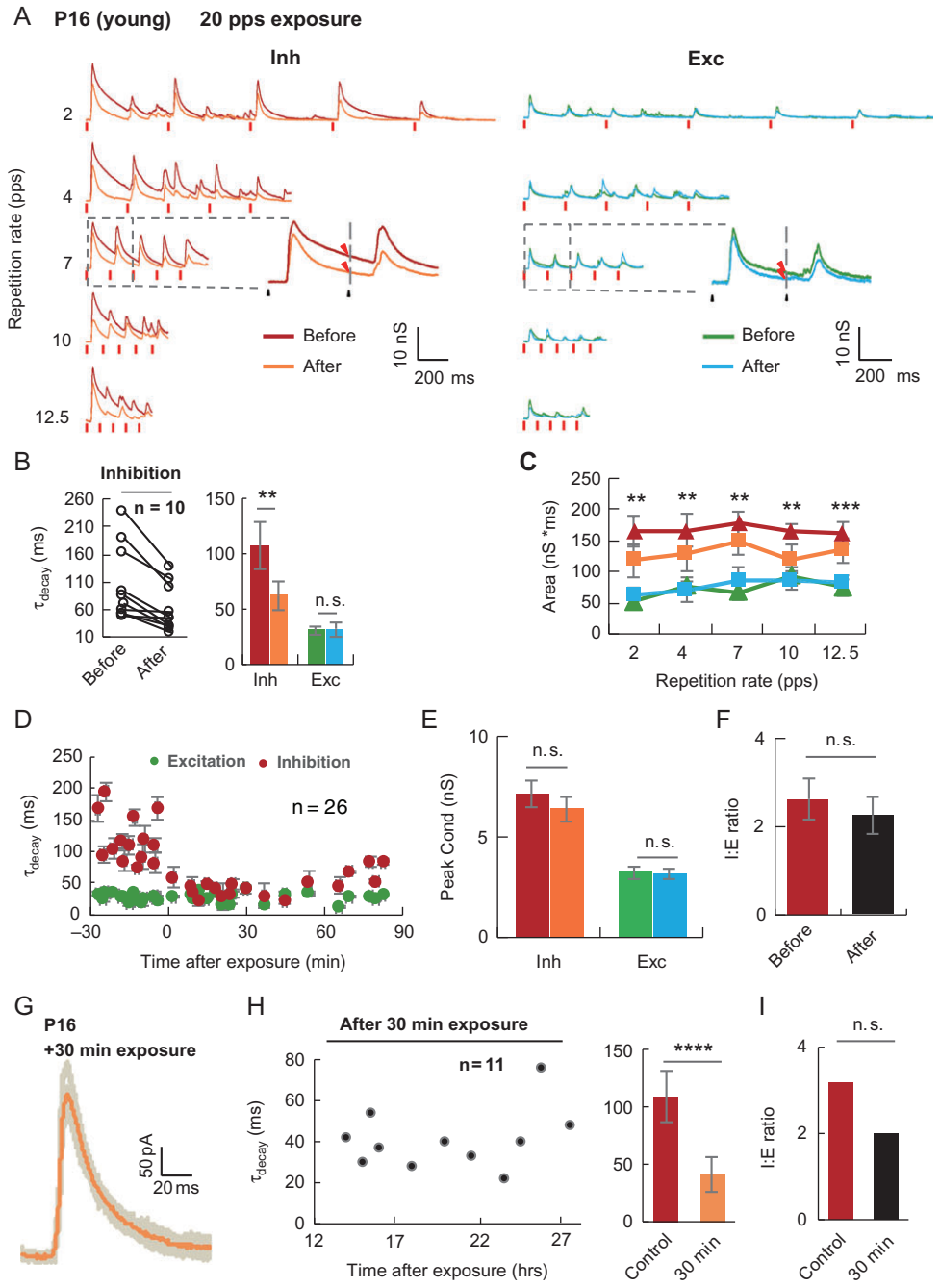

Figure 8. Exposure weakens the summation of inhibition in the developing A1. (*A*) Synaptic temporal Inh and Exc of a P16 neuron evoked before and after 20 pps exposure. Insets, magnified view of synaptic conductance. (*B*) Left, paired comparison of inhibition τ_{decay} before and after 20 pps exposure. Right, average inhibition and excitation τ_{decay} before and after exposure, $n = 10$. Wilcoxon matched-pairs signed-rank test (**$P < 0.01$; n.s. $P > 0.05$). (*C*) Comparison of normalized integral area in young A1 before and after 20 pps exposure, $n = 10$. One-way ANOVA with Bonferroni post-hoc test (**$P < 0.01$; ***$P < 0.001$). (*D*) Effective time course of 5 min of exposure on the shortening of inhibition duration. Red dots, inhibition; green dots, excitation, $n = 26$. (*E*, *F*) Effect of exposure on peak conductance and the *I*:*E* ratio, $n = 10$. Wilcoxon matched-pairs signed-rank test (n.s. $P > 0.05$). (*G*) Example inhibitory synaptic responses of a P16 neuron, recorded 18 h after 30 min of exposure. Gray, superimposed traces; orange, average trace. (*H*) Effective time course of 30 min of exposure on the shortening of inhibition duration, $n = 11$. Left, τ_{decay} at a series of time points after exposure; right, average τ_{decay} of control and exposure groups; control, $n = 15$; exposure, $n = 8$. Mann–Whitney *U*-test (****$P < 0.0001$). (*I*) *I*:*E* ratio of control and exposure groups. Control, $n = 15$; exposure, $n = 8$. Mann–Whitney *U*-test (n.s. $P > 0.05$). Data are means ± SEM (error bars).

identified a specific role of inhibition in shaping the developmental improvement of temporal processing abilities of auditory cortical neurons. The role of inhibition in developmental plasticity of sensory cortices has been extensively studied (Fagiolini et al. 2004; Froemke and Jones 2011; Le Magueresse and Monyer 2013). However, those studies focused on cortical frequency map organization. Temporal features, another fundamental component of sensory stimuli, are not clearly topographically processed in the cortex, and the factors accounting for their developmental plasticity have remained unclear. Here, we provide direct evidence showing that changes in inhibition are involved in developmental plasticity of cortical temporal processing.

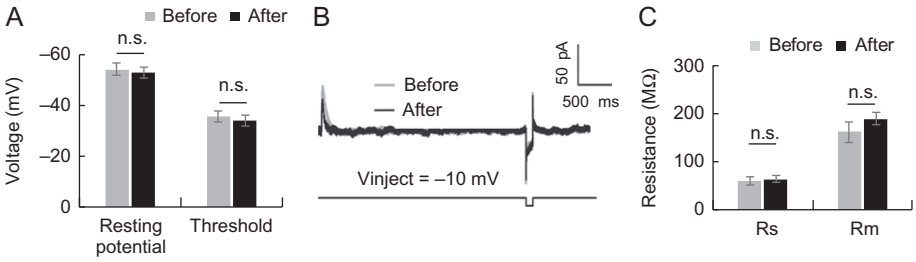

Figure 9. Exposure does not have significant effect on intrinsic properties. (*A*) Resting membrane potential and firing threshold before and after 20 pps exposure, $n = 7$. (*B*) Measurement of series and input resistances before and after 20 pps exposure. Example trace from a P15 neuron, clamped at 0 mV, in response to a noise pulse of 70 dB at 0 s and −10 mv voltage pulse injection at 3 s. Green, inhibitory response before exposure; black, inhibitory response after exposure; bottom trace, voltage injection. (*C*) Series (Rs) and input resistance (Rm) before and after 20 pps exposure. Data are means ± SEM (error bars). Statistical analysis in (*B*) is the paired *t*-test (n.s. $P > 0.05$), and in (*C*) is the Wilcoxon matched-pairs signed-rank test (n.s. $P > 0.05$).

Correlated decreases in membrane time constant of the postsynaptic pyramidal neurons may, in part, contribute to the significantly longer inhibitory duration in the developing A1. However, higher expression level of slow $GABA_A$ receptor subunits in the cortex may be the main factor (Laurie et al. 1992; Gingrich et al. 1995; Mody and Pearce 2004; Ing and Poulter 2007; Kotak et al. 2008; Xu et al. 2010). Interestingly, an in-vivo study reported that the application of $GABA_A$ receptor antagonist to the cortex did not have significant effect on the stronger forward-masking patterns in the developing A1, suggesting that $GABA_B$ receptors might play a role (Chang et al. 2005). An alternative interpretation for this discrepancy is that Chang et al. may have blocked GABA broadly and on many neurons, thus, affecting larger areas of microcircuitry, whereas in-vitro studies may have affected only the inhibition to a single neuron, relying on their measurements in individual neurons and the accepted models of how excitation and inhibition interact to produce membrane potential. We noticed that the duration of inhibition in in-vitro studies is significantly shorter than what we observed in the intact developing A1. These differences may reflect the temporal integration of synaptic inputs from various subtypes of inhibitory neurons in intact neural network, but not the activation of postsynaptic $GABA_B$Rs because we used cesium and QX-314 in our intracellular solution to isolate synaptic currents, which largely blocks $GABA_B$Rs (Oswald et al. 2009; Takesian et al. 2010). An earlier in-vitro study has suggested that presynaptic $GABA_B$R might play a role in the maturation of auditory cortical temporal processing (Takesian et al. 2010). In addition, the mechanisms underlying exposure-induced shortening of inhibitory duration are also unknown. To fully address these questions, further in-vivo pharmacological experiments will be necessary.

It is interesting to find that, compared with RS neurons, the stimulus-following ability of FS neurons does not change much during development. RS neurons in the developing cortex are actually more excitable than FS neurons (Oswald and Reyes 2008, 2011). In addition, given the well-characterized feed-forward thalamocortical projection system, our data suggest that, in the developing A1, thalamic inputs that evoked reliable temporal responses in FS neurons are capable of driving faithful temporal responses in RS neurons as well. Therefore, difference in intracortical inhibitory conductance received by FS and RS neurons may account for the contrast in temporal responses. Indeed, Pfeffer et al. (2013) reported that, although FS neurons are also innervated by inhibitory neurons, the overall inhibitory charges received by FS neurons are less than those received by RS neurons. This could potentially account for the contrast between temporal properties of FS and RS neurons in the developing A1.

In the developing visual cortex, inhibition is gradually strengthened to open and close the critical period for ocular dominance plasticity (Hensch et al. 1998). In intact developing A1, we did not observe significant developmental change in the strength of inhibition, which is generally consistent with previous findings in vivo (Dorrn et al. 2010; Sun et al. 2010). Nonetheless, we did observe a trend of decrease in the level of inhibition, which was also reported in a recent in-vitro study (Oswald and Reyes 2011). The critical period for ocular dominance plasticity in the mouse visual cortex begins at around P28 (Gordon and Stryker 1996), whereas the time point for auditory temporal processing plasticity begins immediately after hearing onset, P12. This large difference in critical period onset between the visual and ACx may reflect different expression levels of GABA receptors throughout the time course of maturation (Laurie et al. 1992; Fritschy et al. 1999).

Our data support the idea that even short periods of sound exposure in young animals can alter the properties of sound-evoked responses. It is known that long periods of altered sensory environments affect the development of ACx (Kotak et al. 2008); that the temporal properties of cortical responses can be altered by sound exposure paired with nucleus basalis stimulation (Kilgard and Merzenich 1998); that even in-vivo very short periods of sound exposure paired with nucleus basalis stimulation can alter sound-evoked responses (Bakin and Weinberger 1996; Froemke et al. 2007). More recently, Dorrn et al. (2010) reported that, even without pairing sensory stimuli with nucleus basalis stimulation, short periods of exposure could refine the frequency tuning of inhibition and promote the establishment of *E–I* balance in the developing A1. In contrast, Sun et al. (2010) reported that *E–I* balance is established from the very beginning of hearing onset. Although the focus of the present study is not *E–I* balance and frequency tuning, we showed that inhibition in the developing A1 is indeed sensitive to acoustic experience. In the study by Dorrn et al. (2010), exposure to sound patterns did not result in a significant decrease in inhibitory duration, in contrast to our observations here. The reason for this discrepancy may be related to the faster repetition rate for the exposure used in our study. Overall, we presented a series of experiments showing that changes in repetition following ability, inhibitory duration, and membrane potential can be reliably induced for both short and longer exposures.

There may be a limitation on generalizing the implication of our results. In this study, to avoid the potential influences of variance in response threshold, stimulus intensity was set at 20 dB above the threshold of each individual neuron recorded. However, we observed a systematic decrease in spiking

threshold from 40–60 dB at P12 to 20–30 dB in adults, so the difference in the duration of inhibition between the 2 age groups might not be observed if absolute sound levels had been used. However, Dorrn et al. (2010) did show examples that are in line with the observed changes in inhibitory duration between young and adult animals. Furthermore, the observed developmental changes in relative onset latency of inhibition and excitation are compatible with the study by Dorrn et al. (2010).

There is a caveat in the interpretation of our whole-cell result. We were using single point voltage-clamp recording to estimate synaptic conductance of cells with extended dendritic trees. Under this condition, cells may not be well voltage-clamped beyond the first 20–50 μm of the dendritic tree (Spruston et al. 1993; Williams and Mitchell 2008). However, our findings are generally consistent with previous findings in vitro, and the voltage-clamp quality in our study was reasonably good, based on the linearity of the *I–V* curves. Moreover, so far, in-vivo whole-cell voltage-clamp recording is still the only approach that allows a direct measure of synaptic inputs in live animals, and it has been widely used to study circuitry properties in sensory systems (Brecht and Sakmann 2002; Wehr and Zador 2003; Atallah and Scanziani 2009; Dorrn et al. 2010; London et al. 2010; Poo and Isaacson 2011; Kuo and Wu 2012; Li et al. 2013). Therefore, this approach may still be valid to shed some light on the synaptic mechanisms underlying the development of auditory cortical temporal processing.

Supplementary Material

Supplementary material are available at *Cerebral Cortex* online.

Author Contributions

K.Y. conceived the experiments, D.C., R.H., M.L., F.X., L.Y., Y.Z., J.Y., Y.W., Y.Y., and K.Y. performed the experiments, D.C., R.H., M.L., Y.Z., L.Z., and K.Y. performed data analysis, D.C., M.L., and K.Y. prepared the figures, and D.C., C.E.S., and K.Y. wrote the manuscript.

Funding

National Natural Science Foundation of China (20131351192, 20151311567).

Notes

We thank P. Cao, E.F. Chang, H.L. Hu, G.S. Liu, M.M. Luo, B.J. Malone, X. Wang and Y. Zuo for comments and discussion, and thank C.J. Cui, B. Hong, F. Hu, X.D. Liu, Z.X. Liu, Y. Liu, Y.S. Shu, W.B. Tang, L.P. Yin, L.N. Zhao, and J.E. Zhang for technical assistance. *Conflict of Interest*: None declared.

References

Ahissar E, Nagarajan S, Ahissar M, Protopapas A, Mahncke H, Merzenich MM. 2001. Speech comprehension is correlated with temporal response patterns recorded from auditory cortex. Proc Natl Acad Sci USA. 98:13367–13372.

Atallah BV, Scanziani M. 2009. Instantaneous modulation of gamma oscillation frequency by balancing excitation with inhibition. Neuron. 62:566–577.

Bakin JS, Weinberger NM. 1996. Induction of a physiological memory in the cerebral cortex by stimulation of the nucleus basalis. Proc Natl Acad Sci USA. 93:11219–11224.

Bao S, Chang EF, Woods J, Merzenich MM. 2004. Temporal plasticity in the primary auditory cortex induced by operant perceptual learning. Nat Neurosci. 7:974–981.

Barbour DL, Callaway EM. 2008. Excitatory local connections of superficial neurons in rat auditory cortex. J Neurosci. 28: 11174–11185.

Barkat TR, Polley DB, Hensch TK. 2011. A critical period for auditory thalamocortical connectivity. Nat Neurosci. 14: 1189–1194.

Brecht M, Sakmann B. 2002. Whisker maps of neuronal subclasses of the rat ventral posterior medial thalamus, identified by whole-cell voltage recording and morphological reconstruction. J Physiol. 538:495–515.

Cardin JA, Palmer LA, Contreras D. 2007. Stimulus feature selectivity in excitatory and inhibitory neurons in primary visual cortex. J Neurosci. 27:10333–10344.

Chang EF, Bao S, Imaizumi K, Schreiner CE, Merzenich MM. 2005. Development of spectral and temporal response selectivity in the auditory cortex. Proc Natl Acad Sci USA. 102:16460–16465.

Chang EF, Merzenich MM. 2003. Environmental noise retards auditory cortical development. Science. 300:498–502.

Cruikshank SJ, Weinberger NM. 1996. Receptive-field plasticity in the adult auditory cortex induced by Hebbian covariance. J Neurosci. 16:861–875.

de Villers-Sidani E, Chang EF, Bao S, Merzenich MM. 2007. Critical period window for spectral tuning defined in the primary auditory cortex (A1) in the rat. J Neurosci. 27:180–189.

Dorrn AL, Yuan K, Barker AJ, Schreiner CE, Froemke RC. 2010. Developmental sensory experience balances cortical excitation and inhibition. Nature. 465:932–936.

Dykes RW, Lamour Y, Diadori P, Landry P, Dutar P. 1988. Somatosensory cortical neurons with an identifiable electrophysiological signature. Brain Res. 441:45–58.

Fagiolini M, Fritschy JM, Low K, Mohler H, Rudolph U, Hensch TK. 2004. Specific GABAA circuits for visual cortical plasticity. Science. 303:1681–1683.

Feldman DE. 2009. Synaptic mechanisms for plasticity in neocortex. Annu Rev Neurosci. 32:33–55.

Fritschy JM, Meskenaite V, Weinmann O, Honer M, Benke D, Mohler H. 1999. GABAB-receptor splice variants GB1a and GB1b in rat brain: developmental regulation, cellular distribution and extrasynaptic localization. Eur J Neurosci. 11: 761–768.

Froemke RC, Jones BJ. 2011. Development of auditory cortical synaptic receptive fields. Neurosci Biobehav Rev. 35:2105–2113.

Froemke RC, Merzenich MM, Schreiner CE. 2007. A synaptic memory trace for cortical receptive field plasticity. Nature. 450:425–429.

Gingrich KJ, Roberts WA, Kass RS. 1995. Dependence of the GABAA receptor gating kinetics on the alpha-subunit isoform: implications for structure-function relations and synaptic transmission. J Physiol. 489(Pt 2):529–543.

Gordon JA, Stryker MP. 1996. Experience-dependent plasticity of binocular responses in the primary visual cortex of the mouse. J Neurosci. 16:3274–3286.

Gray CM, McCormick DA. 1996. Chattering cells: superficial pyramidal neurons contributing to the generation of synchronous oscillations in the visual cortex. Science. 274:109–113.

Hackett TA, Guo Y, Clause A, Hackett NJ, Garbett K, Zhang P, Polley DB, Mirnics K. 2015. Transcriptional maturation of the mouse auditory forebrain. BMC Genomics. 16:606.

Hensch TK. 2005. Critical period plasticity in local cortical circuits. Nat Rev Neurosci. 6:877–888.

Hensch TK, Fagiolini M, Mataga N, Stryker MP, Baekkeskov S, Kash SF. 1998. Local GABA circuit control of experience-dependent plasticity in developing visual cortex. Science. 282:1504–1508.

Imaizumi K, Priebe NJ, Sharpee TO, Cheung SW, Schreiner CE. 2010. Encoding of temporal information by timing, rate, and place in cat auditory cortex. PLoS One. 5:e11531.

Ing T, Poulter MO. 2007. Diversity of GABA(A) receptor synaptic currents on individual pyramidal cortical neurons. Eur J Neurosci. 25:723–734.

Isaacson JS, Scanziani M. 2011. How inhibition shapes cortical activity. Neuron. 72:231–243.

Joris PX, Schreiner CE, Rees A. 2004. Neural processing of amplitude-modulated sounds. Physiol Rev. 84:541–577.

Kanwal JS, Matsumura S, Ohlemiller K, Suga N. 1994. Analysis of acoustic elements and syntax in communication sounds emitted by mustached bats. J Acoust Soc Am. 96:1229–1254.

Khavarghazalani B, Farahani F, Emadi M, Hosseni Dastgerdi Z. 2016. Auditory processing abilities in children with chronic otitis media with effusion. Acta Otolaryngol. 136:456–459.

Kilgard MP, Merzenich MM. 1998. Plasticity of temporal information processing in the primary auditory cortex. Nat Neurosci. 1:727–731.

Kim H, Bao S. 2009. Selective increase in representations of sounds repeated at an ethological rate. J Neurosci. 29: 5163–5169.

Kotak VC, Takesian AE, Sanes DH. 2008. Hearing loss prevents the maturation of GABAergic transmission in the auditory cortex. Cereb Cortex. 18:2098–2108.

Kuhl PK, Andruski JE, Chistovich IA, Chistovich LA, Kozhevnikova EV, Ryskina VL, Stolyarova EI, Sundberg U, Lacerda F. 1997. Cross-language analysis of phonetic units in language addressed to infants. Science. 277:684–686.

Kullmann DM, Moreau AW, Bakiri Y, Nicholson E. 2012. Plasticity of inhibition. Neuron. 75:951–962.

Kuo RI, Wu GK. 2012. The generation of direction selectivity in the auditory system. Neuron. 73:1016–1027.

Laurie DJ, Seeburg PH, Wisden W. 1992. The distribution of 13 GABAA receptor subunit mRNAs in the rat brain. II. Olfactory bulb and cerebellum. J Neurosci. 12:1063–1076.

Le Magueresse C, Monyer H. 2013. GABAergic interneurons shape the functional maturation of the cortex. Neuron. 77: 388–405.

Li YT, Ibrahim LA, Liu BH, Zhang LI, Tao HW. 2013. Linear transformation of thalamocortical input by intracortical excitation. Nat Neurosci. 16:1324–1330.

Liu RC, Miller KD, Merzenich MM, Schreiner CE. 2003. Acoustic variability and distinguishability among mouse ultrasound vocalizations. J Acoust Soc Am. 114:3412–3422.

London M, Roth A, Beeren L, Hausser M, Latham PE. 2010. Sensitivity to perturbations in vivo implies high noise and suggests rate coding in cortex. Nature. 466:123–127.

Mauk MD, Buonomano DV. 2004. The neural basis of temporal processing. Annu Rev Neurosci. 27:307–340.

Mody I, Pearce RA. 2004. Diversity of inhibitory neurotransmission through GABA(A) receptors. Trends Neurosci. 27: 569–575.

Monier C, Chavane F, Baudot P, Graham LJ, Fregnac Y. 2003. Orientation and direction selectivity of synaptic inputs in visual cortical neurons: a diversity of combinations produces spike tuning. Neuron. 37:663–680.

Moore AK, Wehr M. 2013. Parvalbumin-expressing inhibitory interneurons in auditory cortex are well-tuned for frequency. J Neurosci. 33:13713–13723.

Nagarajan S, Mahncke H, Salz T, Tallal P, Roberts T, Merzenich MM. 1999. Cortical auditory signal processing in poor readers. Proc Natl Acad Sci USA. 96:6483–6488.

Nagarajan SS, Cheung SW, Bedenbaugh P, Beitel RE, Schreiner CE, Merzenich MM. 2002. Representation of spectral and temporal envelope of twitter vocalizations in common marmoset primary auditory cortex. J Neurophysiol. 87:1723–1737.

Niell CM, Stryker MP. 2008. Highly selective receptive fields in mouse visual cortex. J Neurosci. 28:7520–7536.

Oswald AM, Doiron B, Rinzel J, Reyes AD. 2009. Spatial profile and differential recruitment of GABAB modulate oscillatory activity in auditory cortex. J Neurosci. 29:10321–10334.

Oswald AM, Reyes AD. 2008. Maturation of intrinsic and synaptic properties of layer 2/3 pyramidal neurons in mouse auditory cortex. J Neurophysiol. 99:2998–3008.

Oswald AM, Reyes AD. 2011. Development of inhibitory timescales in auditory cortex. Cereb Cortex. 21:1351–1361.

Park MH, Won JH, Horn DL, Rubinstein JT. 2015. Acoustic temporal modulation detection in normal-hearing and cochlear implanted listeners: effects of hearing mechanism and development. J Assoc Res Otolaryngol. 16:389–399.

Pfeffer CK, Xue M, He M, Huang ZJ, Scanziani M. 2013. Inhibition of inhibition in visual cortex: the logic of connections between molecularly distinct interneurons. Nat Neurosci. 16:1068–1076.

Polley DB, Read HL, Storace DA, Merzenich MM. 2007. Multiparametric auditory receptive field organization across five cortical fields in the albino rat. J Neurophysiol. 97: 3621–3638.

Polley DB, Thompson JH, Guo W. 2013. Brief hearing loss disrupts binaural integration during two early critical periods of auditory cortex development. Nat Commun. 4:2547.

Ponton CW, Don M, Eggermont JJ, Waring MD, Kwong B, Masuda A. 1996. Auditory system plasticity in children after long periods of complete deafness. Neuroreport. 8:61–65.

Ponton CW, Moore JK, Eggermont JJ. 1999. Prolonged deafness limits auditory system developmental plasticity: evidence from an evoked potentials study in children with cochlear implants. Scand Audiol Suppl. 51:13–22.

Poo C, Isaacson JS. 2011. A major role for intracortical circuits in the strength and tuning of odor-evoked excitation in olfactory cortex. Neuron. 72:41–48.

Rosen S. 1992. Temporal information in speech: acoustic, auditory and linguistic aspects. Philos Trans R Soc Lond B Biol Sci. 336:367–373.

Sanes DH, Kotak VC. 2011. Developmental plasticity of auditory cortical inhibitory synapses. Hear Res. 279:140–148.

Shannon RV, Zeng FG, Kamath V, Wygonski J, Ekelid M. 1995. Speech recognition with primarily temporal cues. Science. 270:303–304.

Shepherd RK, Hartmann R, Heid S, Hardie N, Klinke R. 1997. The central auditory system and auditory deprivation: experience with cochlear implants in the congenitally deaf. Acta Otolaryngol Suppl. 532:28–33.

Singh NC, Theunissen FE. 2003. Modulation spectra of natural sounds and ethological theories of auditory processing. J Acoust Soc Am. 114:3394–3411.

Spruston N, Jaffe DB, Williams SH, Johnston D. 1993. Voltage- and space-clamp errors associated with the measurement of electrotonically remote synaptic events. J Neurophysiol. 70:781–802.

Sun QQ. 2007. The missing piece in the 'use it or lose it' puzzle: is inhibition regulated by activity or does it act on its own accord? Rev Neurosci. 18:295–310.

Sun YJ, Kim YJ, Ibrahim LA, Tao HW, Zhang LI. 2013. Synaptic mechanisms underlying functional dichotomy between intrinsic-bursting and regular-spiking neurons in auditory cortical layer 5. J Neurosci. 33:5326–5339.

Sun YJ, Wu GK, Liu BH, Li P, Zhou M, Xiao Z, Tao HW, Zhang LI. 2010. Fine-tuning of pre-balanced excitation and inhibition during auditory cortical development. Nature. 465:927–931.

Takesian AE, Kotak VC, Sanes DH. 2010. Presynaptic GABA(B) receptors regulate experience-dependent development of inhibitory short-term plasticity. J Neurosci. 30:2716–2727.

Takesian AE, Kotak VC, Sanes DH. 2012. Age-dependent effect of hearing loss on cortical inhibitory synapse function. J Neurophysiol. 107:937–947.

Tallal P, Miller SL, Bedi G, Byma G, Wang X, Nagarajan SS, Schreiner C, Jenkins WM, Merzenich MM. 1996. Language comprehension in language-learning impaired children improved with acoustically modified speech. Science. 271: 81–84.

Tan AY, Zhang LI, Merzenich MM, Schreiner CE. 2004. Tone-evoked excitatory and inhibitory synaptic conductances of primary auditory cortex neurons. J Neurophysiol. 92:630–643.

Temple E, Poldrack RA, Salidis J, Deutsch GK, Tallal P, Merzenich MM, Gabrieli JD. 2001. Disrupted neural responses to phonological and orthographic processing in dyslexic children: an fMRI study. Neuroreport. 12:299–307.

Wang X, Merzenich MM, Beitel R, Schreiner CE. 1995. Representation of a species-specific vocalization in the primary auditory cortex of the common marmoset: temporal and spectral characteristics. J Neurophysiol. 74:2685–2706.

Wehr M, Zador AM. 2003. Balanced inhibition underlies tuning and sharpens spike timing in auditory cortex. Nature. 426: 442–446.

Williams SR, Mitchell SJ. 2008. Direct measurement of somatic voltage clamp errors in central neurons. Nat Neurosci. 11: 790–798.

Wright BA, Lombardino LJ, King WM, Puranik CS, Leonard CM, Merzenich MM. 1997. Deficits in auditory temporal and spectral resolution in language-impaired children. Nature. 387: 176–178.

Xu J, Yu L, Cai R, Zhang J, Sun X. 2010. Early continuous white noise exposure alters auditory spatial sensitivity and expression of GAD65 and GABAA receptor subunits in rat auditory cortex. Cereb Cortex. 20:804–812.

Zhao C, Kao JP, Kanold PO. 2009. Functional excitatory microcircuits in neonatal cortex connect thalamus and layer 4. J Neurosci. 29:15479–15488.

Zhou X, Merzenich MM. 2008. Enduring effects of early structured noise exposure on temporal modulation in the primary auditory cortex. Proc Natl Acad Sci USA. 105: 4423–4428.